ISSN 2594-4711 vol. 17, num. 1 (2017)

BIOCARBONS AS NANOCATALYSTS SUPPORT AND SUPERCAPACITOR ELECTRODES *

Elen Leal da Silva [1]
Martina Cadorin [2]
Andrés Cuña [3]
Nestor Tancredi [4]
Célia de Fraga Malfatti [5]

Resumo

Activated nanoporous biocarbon (aNBC) was prepared using *E. grandis* wood as a precursor material. Oxidated activated nanoporous biocarbon (ox-aNBC) sample was obtained from the aNBC by oxidation with nitric acid. The samples were tested as Pt nanoparticles catalysts support for ethanol oxidation reaction and as electrode materials for supercapacitors. The porous structure, chemical properties, and the structural and morphological characteristic of the materials were correlated with their electrochemical behaviour. Biocarbon materials showed similar high specific surface area. The oxidation treatment increases the content of the oxygenated and nitrogenated surface functional groups but without appreciably change in the nanostructure characteristic. The aNBC supported Pt nanocatalyst has better electrocatalytic performance for EOR. Oxygenated functional groups have a marked effect on the supercapacitors electrode behaviour, increasing the total electrical capacitance by pseudocapacitive contribution, but with a negative effect on the cell electrical resistance and cell response time.

Palavras-chave: Ethanol oxidation; Supercapacitor; Biocarbon; Nanocatalyst;

BIOCARVÃO COMO SUPORTE PARA NANOCATALISADORES E ELETRODOS PARA SUPERCAPACITOR

Abstract

Biocarvão ativado nanoporoso (aNBC) foi preparado usando a madeira *E.grandis* como material precursor. Biocarvão ativado nanoporoso oxidadado (ox-aNBC) foi obtido do aNBC por oxidação com ácido nítrico. As amostras foram testadas como suporte para nanocatalisadores de Pt para eletro-oxidação do etanol e como material para eletrodo de supercapacitores. A estrutura porosa, propriedades químicas, e as características estruturais e morfológicas foram correlacionadas com os seus comportamentos eletroquímicos. Ambos materiais apresentaram alta área de superfície específica. O tratamento de oxidação aumenta o conteúdo de grupos funcionais oxigenados e nitrogenados na superfície, mas sem mudança apreciável na característica nanoestrutural. O aNBC como suporte para nanocatalisadores de Pt tem um melhor desempenho eletrocatalítico na reação de oxidação do etanol. Os grupos funcionais oxigenados têm um efeito destaque no comportamento como eletrodo de supercapacitor, aumentando a capacitância elétrica total por contribuição pseudocapacitiva, mas com um efeito negativo na resistência elétrica da célula e no seu tempo de resposta.

Keywords: Oxidação do etanol; Supercapacitor; Biocarvão; Nanocatálise;

[1] *Pós-doutoranda – Laboratório de Pesquisa em Corrosão – LAPEC- Departamento de Metalurgia - UFRGS.*
[2] *Graduanda em Engenharia Metalúrgica – Laboratório de Pesquisa em Corrosão – LAPEC-UFRGS*
[3] *Prof. Dr. Facultad de Química - Cátedra de Fisicoquímica – UdelaR – Montevideo.*
[4] *Prof. Dr. Facultad de Química - Cátedra de Fisicoquímica – UdelaR – Montevideo.*
[5] *Profª Dra. Laboratório de Pesquisa em Corrosão – LAPEC- Departamento de Metalurgia – UFRGS.*

** Contribuição técnica ao 72º Congresso Anual da ABM – Internacional e ao 17º ENEMET - Encontro Nacional de Estudantes de Engenharia Metalúrgica, de Materiais e de Minas, parte integrante da ABM Week, realizada de 02 a 06 de outubro de 2017, São Paulo, SP, Brasil.*

ISSN 2594-4711 vol. 17, num. 1 (2017)

1 INTRODUCTION

Direct ethanol fuel cells (DEFCs) are based on ethanol oxidation reaction (EOR) at low temperature and they constitute an alternative energy conversion system [1]. Besides, supercapacitors are promising electrochemical energy storage devices with important advantages over batteries, including higher power density and larger number of charge/discharge cycles. Carbon materials, including nanostructured carbon, are the most widely used materials for supercapacitor electrodes [2,3] and as nanocatalysts support for fuel cells [4,5] because they satisfy all the requirements for these applications: high specific surface area, nanoporosity, high electrical conductivity, electrochemical stability and moderate low cost. Activated nanoporous carbons are currently prepared from a high carbon content precursor, such as polymer, mineral carbon or biomass waste [6]. Biomass waste is a renewable source, with low cost, available in large amounts and can be used for multiple energetic purposes [7,8,9,10]. The use of biomass derived carbons (biocarbons) as active electrode materials for supercapacitors and as nanocatalysts support for EOR has been reported over the last years with promising results [11,12,13,14]. The biomass nature and the activation method determine the nanoporous carbon properties, surface chemistry, electrical conductivity and electrochemical performance of the materials [8, 9, 11, 15]. Furthermore, nanoporous carbon materials may have different types of oxygenated and/or nitrogenated surface functional groups [6]. Some of these functional groups are electrochemically active in acidic electrolyte and can contribute to the total capacitance of the supercapacitor electrode by reversible redox reactions, phenomenon known as pseudocapacitance [2,16]. In addition, these functional groups may have different effects in the degree of dispersion and/or agglomeration of catalyst nanoparticles when used as support and they can also be introduced through different chemical treatments such as nitric acid oxidation [17].

Eucalyptus is a tree cultivated all over the world and has the advantage of its rapid growing. Its wood is currently used for manufacturing furniture and for obtaining cellulose paste, bur also allows the preparation of activated carbons with high microporosity [18].

In this work, Eucalyptus grandis wood dust was chosen as carbon precursor, and activated nanoporous biocarbon (aNBC) was prepared by chemical activation with ZnCl2. To increase the content of oxygenated surface functional groups, oxidized activated nanoporous biocarbon (ox-aNBC) was obtained from the aNBC sample by chemical oxidation with nitric acid. The nanoporous structure characteristic and chemical properties of the prepared materials were determined. Then, aNBC and ox-NBC were tested as Pt nanoparticles catalysts support for EOR and as electrode materials for supercapacitors. The porous structure and chemical properties of the materials were correlated with its electrochemical behaviour.

2 MATERIALS AND METHODS

2.1 Biocarbons preparation and characterization

Activated nanoporous biocarbon (aNBC) was prepared from E. grandis wood by chemical activation with $ZnCl_2$ (activation agent/wood weight ratio = 1/1) at 900 °C for 1 h. Before the activation, the wood was grinded, sifted and then dried at 105 ° C for 24 hours. Oxidized sample (ox-aNBC) was prepared through the oxidation of the aNBC with a 4 mol L^{-1} nitric acid solution for 1.5 h. After the chemical activation and oxidation treatment, the samples were washed with distilled water up to neutral pH of the washing water, and then dried in still air at 105 °C for 24 hours. All the thermal

treatments were carried out in a horizontal Carbolite (CTF 12/75) furnace under a controlled N_2 gas flow. The activation methods used were based on the previous described procedures [6, 11, 14].

The nanoporous structure of the biocarbon materials was characterized by N_2 adsorption/desorption isotherms at 77 K, using a Beckman Coulter SA 3100 equipment. Microporous volume (W_o), microporous surface area (S_{mic}) and the average micropore width (L_0) were determined by the Dubinin-Radushkevich equation and the Dubinin-Stoeckli equation [19]:

$$\boldsymbol{L_0\,(nm) = 10.8/[E_0(kJ\,mol^{-1}) - 11.4]} \quad (1)$$

$$\boldsymbol{S_{mic}(m^2 g^{-1}) = 2000 W_0(cm^3 g^{-1})/L_0(nm)} \quad (2)$$

where E_o is the characteristic energy obtained from the classical Dubinin-Radushkevich isotherm plot.

Elemental composition (nitrogen, hydrogen, carbon and sulfur) was determined with a Thermo Scientific Flash 2000 equipment. Ash content was determined according to ASTM D2866/2011 and the oxygen content was determined by difference. To identify the chemical functional groups on the nanoporous biocarbons materials, samples were analyzed by Fourier Transform Infrared Spectroscopy (FTIRS) using a Shimadzu IRPrestige-2 equipment. For this analysis, the carbon material was diluted in a KBr pellet.

2.2 Electrocatalysts preparation and characterization

Different Pt based electrocatalysts were prepared using aNBC and ox-NBC as support materials. Electrocatalysts synthesis was already explained in a former work [20]. Impregnation/reduction method was employed using ethylene glycol as reduction agent and $H_2PtCl_6.6H_2O$ salt as catalyst precursor. Adequate amounts of support and salt were mixed together to obtain electrocatalysts with a metal charge of 40 wt. %.

X-Ray diffraction analysis was performed with a Philips, X'Pert MPD equipment, operating with Cu-Kα radiation, generated with 40 kV and 40 mA. X-Ray diffractogram allowed to stablish the crystal structure of the catalyst inside the support. Morphological information for the catalysts was obtained by Transmission electron microscopy analysis (TEM) with a FEI Tecnai Spirit Biotwin G2 TEM, operating at 100 kV.

The porous structure and the elemental analysis of the prepared electrocatalysts were determined with the same equipments and the same methods previously described. Using a three-electrode cell, with platinum wire as counter-electrode and saturated calomel electrode (SCE) as reference, cyclic voltammetry was carried out to determine the electrochemical behaviour of the catalyst in 1.0 mol L^{-1} ethanol + 0.5 mol L^{-1} H_2SO_4 solution. As working electrode, a graphite disk was used with a geometric area of 0.29 cm^2, which was coated with a mixture of catalyst powder in Nafion®. The scan rate used was 20 mV s^{-1}, applied between the potential range of -0.03 to 0.96 V [21]. To eliminate the oxygen present in the medium, nitrogen was purged for 10 minutes before the experiment. All electrochemical measurements were performed at 25 °C, on a potentiostat/ galvanostat AUTOLAB PGSTAT 302N.

2.3 Supercapacitor electrodes preparation and characterization.

Two-electrode Swagelok®-type cells having two tantalum rods as current collectors were used for galvanostatic charge/discharge and electrochemical impedance spectroscopy (EIS) measurements. A glassy microfiber paper (Whatman 934 AH) was chosen as separator. The electrodes (about 50 mg) were prepared by mixing the nanoporous biocarbon sample (85 wt. %) and polyvinylidene fluoride as a binder (15 wt. %). The two components were mixed and grinded in an agate mortar. Then, cylindrical pellets of 6 mm in diameter and about 2 mm in thickness were obtained after cold pressing at 10 MPa. 2 mol L^{-1} H2SO4 solution was used as electrolyte.

The specific capacitances were determined from galvanostatic charge/discharge curves in the voltage range of 0 V - 1 V at current densities in the range 1 - 150 mA cm^{-2}. The total specific capacitance Cs was determined at each current according to the equation 3:

$$C_S = 2It_d/E_2m \quad (3)$$

where I is the current applied, t_d is the discharge time, E_2 is the voltage range during the discharge, and m is the mass of nanoporous biocarbon material in one electrode. EIS measurements were carried out in the frequency range from 10^{-4} to 106 Hz with perturbation of sinusoidal amplitude of 15 mV (rms) and 10 points per frequency decade [2]. All electrochemical measurements were carried out at the same temperature and with the same equipment described in the previous section.

3 RESULTS AND DISCUSSION

3.1 Porous structure characterization and elemental analysis

The porous structure parameters and the elemental analysis of the samples are shown in Table 1. aNBC has a slightly small micropore volume (W_o) and pore size (L_o), but has slightly higher specific micropore surface area (S_{mic}). These changes in the microporous structure of the aNBC after the nitric acid treatment can be explained by the partial destruction of the pore structure by the oxidation process [6].

Table 1. Porous structure characterization and elemental analysis of the nanoporous biocarbons and electrocatatalysts

	Textural analysis			**Elemental Analysis (mass percentage, dry basis)**					
Sample	W_o ($cm^3\ g^{-1}$)	S_{mic} ($m^2\ g^{-1}$)	Lo (nm)	C	H	N	S	Ash	O*
aNBC	0.48	821	1.17	89.7	0.9	0.1	0.0	0.6	8.7
ox-aNBC	0.49	778	1.26	60.4	1.6	0.6	0.0	0.3	37.7
Pt/aNBC	0.45	741	1.21	70.8	1.1	0.2	0.0	12.2	15.8
Pt/ox-aNBC	0.34	536	1.28	55.8	1.0	0.4	0.0	29.1	13.7

*Determined by difference.

The nitric acid treatment of the aNBC produced a significant increase in the oxygen content (from 8.7 to 37.7 %), and to a lesser extent, an increase in the

nitrogen content (0.1 to 0.6 %), which indicates the effectiveness of the nitric acid treatment in modifying the nanoporous biocarbon surface, in agreement with previous research [22]. This modification results in an increased content of oxygenated and nitrogenated surface functional groups in the oxidized sample, which can be seen in the spectras obtained through Fourier Transform Infrared Spectroscopy (FTIRS), as shown in Figure 2. Only the ox-aNBC sample shows a clear band in 1385 cm^{-1} corresponding to the bending vibration of $-NO_2$ [22] and in

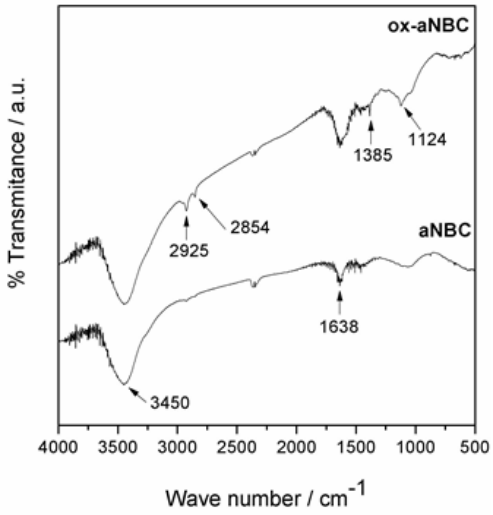

1124 cm^{-1} corresponding to the –C-OH stretching band of carboxyl or hydroxyl functional groups [23]. In the oxidized sample, it can also be seen an increase in the bands located in 1638 cm^{-1}, 2854 cm^{-1} and 2925 cm^{-1}, which could correspond to an increase in the concentration of surface functional groups such as quinone, and to the presence of aliphatic species respectively [23].

Figure 1. FTIR patterns of aNBC and ox-aNBC

The band in 3450 cm^{-1} in both spectra is associated with O-H stretching vibrations of hydroxylic groups and chemisorbed water. In summary, from the textural characterization, FTIRS and chemical analysis of the samples, it can be said that the nitric acid treatment performed to the aNBC sample has succeeded in modifying the surface chemistry composition, increasing the content of oxygenated and nitrogenated functional groups, although with a less incidence in the nanoporous structure of the biocarbon.

3.2 Pt nanocatalysts supported on activated nanoporous biocarbons: morphology, structure and electrocatalytic performance.

Figure 3 shows X-ray diffractograms for both electrocatalysts prepared. Peaks at 39°, 46º, 68º, 81º and 87° attributed to the (1 1 1), (2 0 0), (2 2 0), (3 1 1) and (2 2 2) planes which correspond to typical face centered cubic (FCC) crystal structure of crystalline platinum [24,25]. These results confirm the Pt nanoparticle synthesis on both biocarbon's supports.

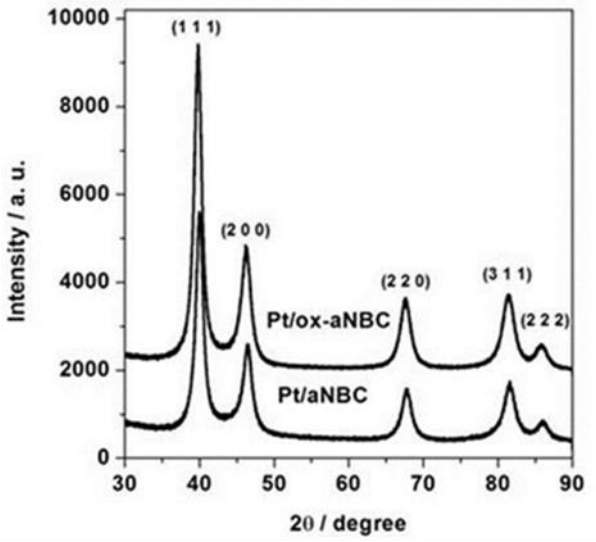

Figure 2. X-ray diffraction patterns of the Pt/aNBC and Pt/ox-aNBC electroctalysts

Pt nanocatalyst distribution in the different nanoporous biocarbon supports and their particle size distribution histograms were obtained from TEM micrographs examination (Figure 4). The nanocatalyst's particles have very similar size for both samples, with average sizes of 3.73 ± 0.75 nm for Pt/aNBC and 3.71 ± 0.93 nm for Pt/ox-aNBC. No clearly difference is observed in the dispersion and agglomeration of the nanocatalyst particles on the support surface. Even so, the Pt metal charge (related with the ash content) in the Pt/ox-aNBC sample is higher than in the Pt/aNB. As showed in Table 1, the ash content is 29.1 and 12.2 % for the oxidized and not oxidized support respectively.

The porous structure parameters are listed in Table 1. S_{mic} and W_o clearly decreased for the Pt/ox-aNBC sample, from 778 to 536 $m^2\ g^{-1}$ and from 0.49 to 0.34 $cm^3\ g^{-1}$ respectively, while for the Pt/aNBC the decrease in the S_{mic} and W_o values were from 841 to 821 $m^2\ g^{-1}$ and from 0.48 to 0.45 $cm^3\ g^{-1}$ respectively. These results may demonstrate an increased porosity occlusion of the oxidized support due to higher nanocatalyst deposition within the pores of the support. This agrees with the higher Pt content determined for the Pt/ox-aNBC sample.

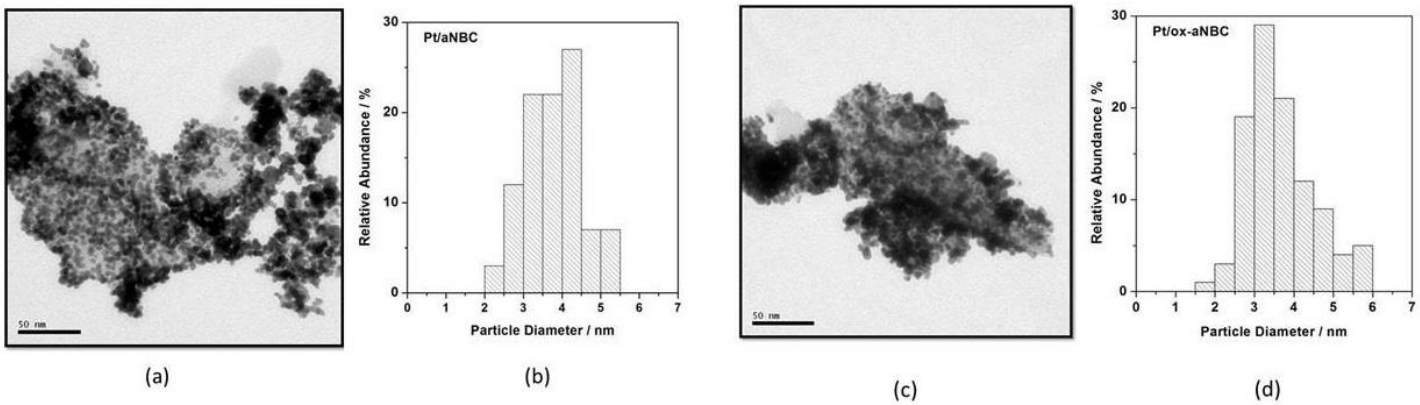

Figure 3. TEM micrographs of the (a) Pt/aNBC and (c) Pt/ox-aNBC electrocatalysts and the histogram of the catalyst particle mean diameter distribution (b) and (d) respectively

Figure 5 shows the cyclic voltammetries obtained for Pt/aNBC and Pt/ox-aNBC electroctatalysts in acidic ethanol solution. These results evidence a good electrocatalytic performance regarding their use for EOR, and thus may be suitable as anode catalyst material in DEFCs.

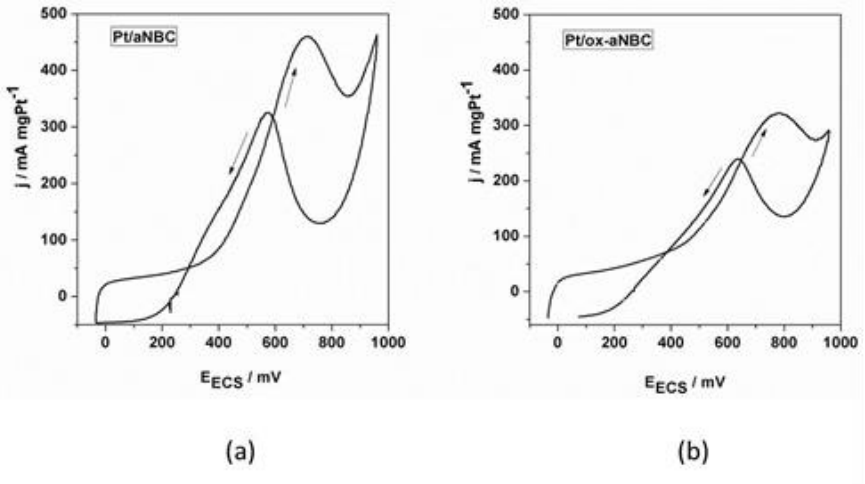

Figure 4. Cyclic voltammograms of different electrocatalysts in 0.5 mol L^{-1} H2SO4 + 1.0 mol L^{-1} ethanol solution at 20 mV s-1 (a) Pt/aNBC and (b) Pt/ox-aNBC

The voltammograms present two oxidation peaks, one in direct scan, and the other in reverse scan. This voltammetric profile has been reported elsewhere [20]. The peak in direct sweep can be related to EOR, whereas the one in reverse sweep could be associated to incompletely oxidized carbonaceous residues on the nanocatalyst surface [26]. Comparing the voltammograms of the different electrocatalysts, the Pt/aNBC electrocatalyst developed a higher current density (j) than the Pt/ox-aNBC electrocatalyst and maximum current density (j_{max}) was 459 mA $mgPt^{-1}$ and 322 mA $mgPt^{-1}$ respectively. Pt/ox-aNBC electrocatalyst showed lower j_{max}, even though it has higher Pt content (see ash content in Table 1). Its lower electrocatalytic performance may be related to a lower electrocatalytic active surface area caused by the higher metal charge in this sample [27]. Also, the onset potential (E_{onset}) determined for the Pt/aNBC electrocatalyst (E_{onset} = 0.33 V) is slightly lower than that determined for the Pt/ox-aNBC electrocatalyst (E_{onset} = 0.38 V).

3.3 Activated nanoporous biocarbons as supercapacitor electrodes

The dependence of the specific (gravimetric) capacitance as a function of the current density is shown in Figure 6 (a). At low current density (1 mA cm^{-2}), the oxidized sample (ox-aNBC) has higher value than the non-oxidized nanoporous biocarbon (aNBC), C_{s1} = 200 F g^{-1} and 175 F g^{-1} respectively. This difference cannot be assigned to textural differences of the materials, since both samples have the same pore size and similar surface areas (see Table 1). If we consider the value of the electrochemical double-layer for similar materials (0.10 F m^{-2} in acidic electrolyte) [2] and the S_{mic} values, the expected value for the electric double-layer capacitance (C_{dl}) can be determined as follow:

$$\boldsymbol{C_{dl}(Fg^{-1}) = S_{mic}(m^2g^{-1})0.10(Fm^{-2})} \quad (4)$$

The C_{dl} is 82.1 F g-1 and 77.8 F g-1 for aNBC and ox-aNBC respectively. The difference between these values and those obtained for the total specific capacitance at 1 mA cm^{-2} (C_{s1}) accounts for the pseudocapacitive contribution. This pseudocapacitive contribution is more important for the oxidized sample (61 % of the total capacitance) than the non-oxidized one (53 %). The presence of reversible

redox reactions in a similar biocarbon material was clearly demonstrated by Cuña et al. [11] by cyclic voltammetry analysis, where the voltammogram obtained for the oxidized sample showed a broad peak between 0.2 V and 0.5 V, assigned to reversible reactions of the surface functional groups, particularly quinone and hydroxyl groups [2, 28]. This is consistent with the elemental analysis and FTIRS results obtained in this work, which demonstrates an increase of these oxygenated functional groups after the oxidative treatment. It has also been reported that carboxyl, hydroxyl and nitro functional groups, can improve the wettability of carbon facilitating the electrolyte accessibility in the carbon pores [29,30]. This will influence the double-layer capacitance that can be obtained, especially in fine-pore high-area materials [29]. These differences also result in a lower capacitance retention (as a percentage of electrical capacitance measured at 1 mA cm^{-2}) of the aNBC sample. As shown in Figure 6 (b), the capacitance retention at 100 mA cm^{-2} is 75 % for the aNBC sample and 49 % for the ox-aNBC.

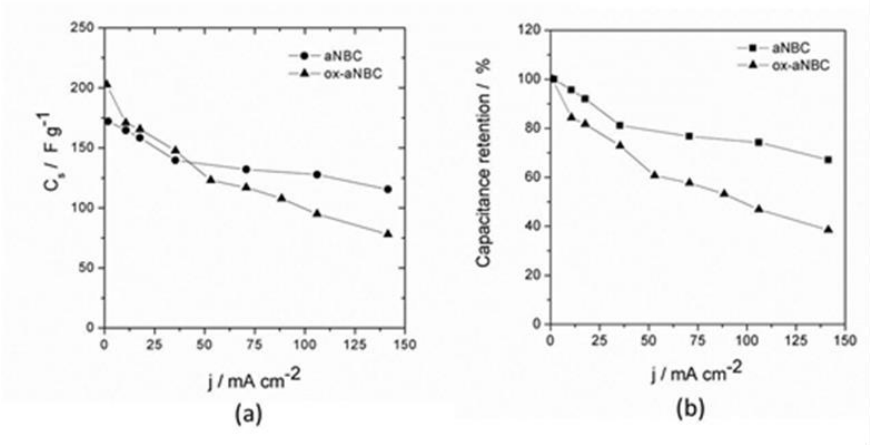

Figure 5. (a) Specific capacitance vs current density for aNBC and ox-aNBC (b) Capacitance retention vs. current density.

In Figure 7, (a) and (c), is shown the Nyquist diagram for the supercapacitor cell using aNBC and ox-aNBC as electrode. From this diagram, the total resistance for the cell (R_T) can be evaluated. This resistance is commonly described as the sum of two resistances, R_a and R_s, where the term R_a (resistance of the arc) corresponds to the sample electrode and current collector-electrode resistance, and resistance R_s is related to the bulk electrolyte resistance [31]. R_s value is very similar for both samples, 1.5 and 1.3 Ω for aNBC and ox-aNBC respectively, since the same electrolyte was used in both systems. The higher value of R_T obtained for the ox-aNBC sample (55.0 Ω) than for aNBC (7.5 Ω), suggests that the introduction of oxygenated functional groups through oxidation makes the material more electrically resistive. The presence of oxygenated groups at the carbon surface and their negative contribution to the electrical conductivity was already reported [32].

For both samples, the variation of C" capacitance as a function of angular frequency, Figure 7 (b) and (d), shows a peak whose frequency at the maximum can be determined. Then, the cell response time (i.e., the minimum time that the cell needs to be charged or discharged) can be calculated as $\tau = 1/\omega_{max}$, where ω_{max} is the angular frequency at the maximum of the C" peak. The cell response time is higher for the cell containing the ox-aNBC (τ = 100 s) than the cell containing the aNBC (τ = 27 s).

ISSN 2594-4711 vol. 17, num. 1 (2017)

The smaller τ value for aNBC can be related to the predominant of double-layer formation, which constitutes a faster electrochemical process [32]. Meanwhile, the higher response time for ox-aNBC sample can be related to the additional redox reactions, enhanced by the presence of the surface functional groups, whose kinetics is slow compared to the double-layer formation [2].

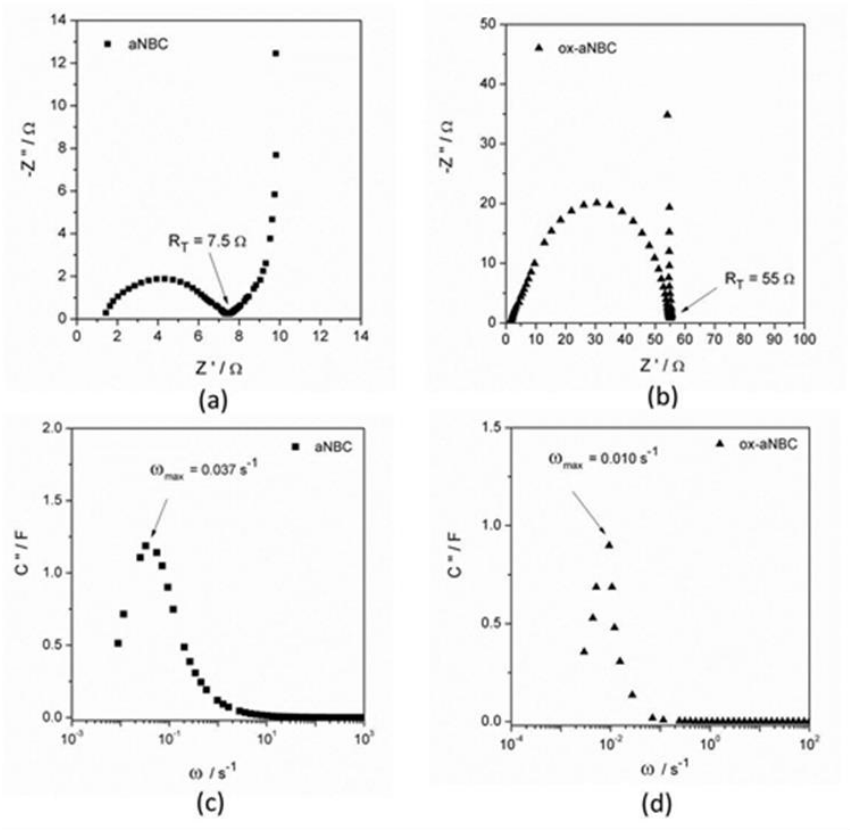

Figure 8. Impedance analysis results. Nyquist diagram for (a) aNBC and (b) ox-NBC; and imaginary capacitance vs. angular frecuency for (c) aNBC and (d) ox-NBC.

4 CONCLUSIONS

The prepared E. grandis wood based nanoporous biocarbon materials, aNBC and ox-aNBC, have good qualities for use as nanocatalyst support for EOR and as supercapacitor electrode. Samples showed similar high specific surface area associated to a nanostructured porosity. The nitric acid oxidation treatment increases the content of the oxygenated and nitrogenated surface functional groups in the sample ox-aNBC, such as quinone, carboxylic and nitro groups. This treatment does not produce an appreciable change in the nanostructure characteristic. These functional groups do not have a clear effect in the degree of dispersion and agglomeration of the Pt nanocatalyst particles when the carbon material is used as electrocatalyst support for electro-oxidation of ethanol. The Pt/aNBC electrocatalyst has better electrocatalytic performance for ethanol electro-oxidation than the Pt/ox-aNBC. The content of oxygenated functional groups has a marked effect in the supercapacitors electrode behavior, increasing the total electrical capacitance by pseudocapacitive contribution but with a negative effect on the cell total electrical resistance and cell response time.

5 AKNOWLEDGEMENT

The present work was carried out with support of CAPES (project CAPES /UdelaR N° 044/2011). A. Cuña thanks the Brazilian CAPES (Bolsista CAPES/Brasil) and E. Leal da Silva thanks the Brazilian CNPq (Bolsista CNPq/Brasil 152027/2016-5 - PDJ).

6 REFERENCES

1 Akhairi MAF and Kamarudin SK. Catalysts in direct ethanol fuel cell (DEFC): An overview. International Journal of Hydrogen Energy. 2016:41:4214-4228.
2 Béguin F and Frąckowiak E. Supercapacitors: Materials, Systems and Applications. Wiley-VCH Verlag GmbH & Co, Weinheim; 2013.
3 Ong YT, Ahmad AL, Zein SHS, Tan SH. A review on carbon nanotubes in an environmental protection and green engineering perspective. Brazilian Journal of Chemical Engineering. 2010:27:227-242.
4 Serp P and Machado B. Nanostructured Carbon Materials for Catalysis. Royal Social of Chemistry, Londres; 2015.
5 Liang J, Zhang Qiao S, Qing (Max) Lu G. Hulicova-Jurcakova D. Carbon-based Catalyst Support in Fuel Cell Applications. Chapter 18. Novel Carbon Adsorbents; 2012.
6 Marsh H and Rodríguez-Reinoso RF. Activated carbons. Elsevier, Oxford, UK; 2006.
7 Kalyani P and Anitha A. Biomass carbon & its prospects in electrochemical energy systems. International Journal of Hydrogen Energy. 2013:38:4034-4045.
8 Kharat DS. Preparing agricultural residue basedadsorbents for removal of dyes from effluents - a review. Brazilian Journal of Chemical Engineering. 2015:32:1-12.
9 Xavier TP, Lira TS, Schettino Jr, MA, Barrozo MAS. A study of pyrolysis of macadamia nut shell: parametric sensitivity analysis of the IPR model. Brazilian Journal of Chemical Engineering. 2016:33:115-122.
10 Virmond E, Rocha JD, Moreira RFPM, José HJ, Valorization of agroindustrial solid residues and residues from biofuelproduction chains by thermochemicalconversion: a review, citing brazil as a case study. Brazilian Journal of Chemical Engineering. 2013:30:197-230.
11 Cuña A, Tancredi N, Bussi J, Barranco V, Centeno TA, Quevedo A, Rojo JM. Influence of wood anisotropy on the Electrical and Electrochemical Performance of Biocarbon Monoliths as Supercapacitor Electrode. Journal of the Electrochemical Society. 2014:161:A1806-A1811.
12 Cuña A, Tancredi N, Bussi J, Deiana C, Sardella MF, Barranco V, Rojo JM. E. grandis as a biocarbons precursor for supercapacitor electrode application. Waste and Biomass Valorization. 2014:5:305-313.
13 Leal da Silva E, Ortega Vega MR, Correa PS, Cuña A, Tancredi N, Malfatti CF. Influence of activated carbon porous texture on catalyst activity for ethanol electro-oxidation. International Journal of Hydrogen Energy. 2014:39:14760-14767.
14 Rufford TE, Hulicova-Jurcakova D, Zhu Z, Lu GQ. Nanoporous carbon electrode from waste coffee beans for high performance supercapacitors. Electrochemistry Communications. 2008:10:1594-1597.
15 Rufford TE, Hulicova-Jurcakova D, Zhu Z, Lu GQ. Microstructure and electrochemical double-layer capacitance of carbon electrodes prepared by zinc chloride activation of sugar cane bagasse. Journal of Power Sources. 2010:195:912-918.
16 Seredycha M, Hulicova-Jurcakovab D, Lub GQ, Bandosza TJ. Surface functional groups of carbons and the effects of their chemical character, density and accessibility to ions on electrochemical performance. Carbon. 2008:46:1475-1488.
17 Shen W, Li Z, Liu Y. Surface Chemical Functional Groups Modification of Porous Carbon. Recent Patents on Chemical Engineering. 2008:1:27-40.

ISSN 2594-4711 vol. 17, num. 1 (2017)

18 Amaya A, Medero N, Tancredi N, Silva H, Deiana C. Activated carbon briquettes from biomass materials. Bioresource Technology. 2007:98:1635-1641.
19 Stoeckli F and Centeno TA. Optimization of the characterization of porous carbons for supercapacitors. Journal of Materials Chemistry A. 2013:1:6865-6873.
20 Correa PS, da Silva EL, da Silva RF, Radtke C, Moreno B, Chinarro, E, CF Malfatti. Effect of decreasing platinum amount in Pt–Sn–Ni alloys supported on carbon as electrocatalysts for ethanol electrooxidation. International Journal of Hydrogen Energy. 2012:37:9314-9323.
21 Jiang L, Sun G, Zhou Z, Zhou W, Xin Q. Preparation and characterization of PtSn/C anode electrocatalysts for direct ethanol fuel cell. Catalysis Today. 2004:93:665-670.
22 Liu MC, Kong LB, Zhang P, Luo YC, Long K. Porous wood carbon monolith for high-performance supercapacitors. Electrochimica Acta. 2012:60:443-448.
23 Biniak S, Szymanski G, Siedlewski J, Swiatkowski A. The characterization of activated carbons with oxygen and nitrogen surface groups. Carbon. 1997:35:1765-1779.
24 Zhou W, Zhou Z, Song S, Li W, Sun G, Tsiakaras P, et al. Pt based anode catalysts for direct ethanol fuel cells. Applied Catalysis B: Environmental. 2003:46:273-285.
25 Chatterjee M, Chatterjee A, Ghosh S, Basumallick I. Electro-oxidation of ethanol and ethylene glycol on carbon-supported nano-Pt and -PtRu catalyst in acid solution. Electrochimica Acta. 2009:54:7299-7304.
26 Kim JH, Choi SM, Nam SH, Seo MH, Choi SH, Kim WB. Influence of Sn content on PtSn/C catalysts for electrooxidation of C1–C3 alcohols: Synthesis, characterization, and electrocatalytic activity. Applied Catalysis B: Environmental. 2008:82:89-102.
27 Watt-Smith MJ, Friedrich JM, Rigby SP, Ralph TR, Walsh FC. Determination of the electrochemically active surface area of Pt/C PEMfuel cell electrodes using different adsorbates. Journal of Physics D: Applied Physics. 2008:41:174004.
28 Sliwak A, Grzyb B, Cwikła, J., Gryglewicz, G., Influence of wet oxidation of herringbone carbon nanofibers on the pseudocapacitance effect. Carbon. 2013:64:324-333.
29 Prabaharan SRS, Vimala R, Zainal Z. Nanostructured mesoporous carbon as electrodes for supercapacitors. Journal of Power Sources. 2006:161:730-736.
30 Kobayashi N, Ogata H, Park KC, Takeuchi K, Endo M. Investigation on capacitive behaviors of porous Ni electrodes for electric double layer capacitors, Electrochimica Acta. 2013:90:408-415.
31 García-Gómez A, Miles P, Centeno TA, Rojo JM. Uniaxially oriented carbon monoliths as supercapacitor electrodes. Electrochimica Acta. 2010:55:8539-8544.
32 Radeke KH, Backhaus KO, Swiatkowski A. Electrical conductivity of activated carbons. Carbon. 1991:29:122-123.
33 Popova A and Christov M. Evaluation of impedance measurements on mild steel corrosion in acid media in the presence of heterocyclic compounds. Corrosion Science. 2006:48:3208-3221.